Cellular/Molecular

Deletion of the GABA$_A$ Receptor α1 Subunit Increases Tonic GABA$_A$ Receptor Current: A Role for GABA Uptake Transporters

Pavel I. Ortinski,[1,2] **Jill R. Turner,**[1,3] **Andrea Barberis,**[2] **Gholam Motamedi,**[4] **Robert P. Yasuda,**[1,3] **Barry B. Wolfe,**[1,3] **Kenneth J. Kellar,**[1,3] **and Stefano Vicini**[1,2]

[1]Interdisciplinary Program in Neuroscience and Departments of Physiology and Biophysics, [3]Pharmacology, and [4]Neurology, Georgetown University School of Medicine, Washington, DC 20007

The loss of more than half the number of GABA$_A$ receptors yet lack of pronounced phenotype in mice lacking the gene for the GABA$_A$ α1 subunit is somewhat paradoxical. We explored the role of tonic GABA$_A$ receptor-mediated current as a target of compensatory regulation in the α1 knock-out ($-/-$) mice. A 62% increase of tonic current was observed in the cerebellar granule cells (CGCs) of α1$^{-/-}$ compared with wild-type ($+/+$) mice along with a 67% increase of baseline current variance. Examination of whole-cell currents evoked by low concentrations of GABA and 4,5,6,7-tetrahydroisoxazolo[5,4-c]pyridin-3-ol suggested no upregulation of α6 and δ subunit-containing GABA$_A$ receptors in the α1$^{-/-}$, confirming previous biochemical studies. Single-channel current openings were on average 32% shorter in the α1$^{-/-}$ neurons. Single-channel conductance and frequency of opening were not different between genotypes. Tonic current induced by application of the GABA transporter GAT-1 blocker NO711 (1-[2([(diphenylmethylene)imino]oxy)ethyl]-1,2,5,6-tetrahydro-3-pyridinecarboxylic acid hydrochloride) was significantly larger in the α1$^{-/-}$, suggesting an increase of ambient GABA concentration. Experiments done with a known concentration of extracellular GABA complemented by a series of biochemical experiments revealed a reduction of GAT activity in α1$^{-/-}$ without an identifiable reduction of GAT-1 or GAT-3 protein. We report increased tonic GABA$_A$ receptor-mediated current in the α1$^{-/-}$ CGCs as a novel compensatory mechanism. Our data establish a role for GABA transporters as regulators of neuronal excitability in this and relevant models and examine other tonic conductance-regulating mechanisms responsible for the adaptive response of the cerebellar network to a deletion of a major synaptic GABA$_A$ receptor subunit.

Key words: GABA$_A$; α1; knock-out; tonic inhibition; GABA transporter; patch-clamp

Introduction

GABA$_A$ receptor α1 subunits are strongly expressed at synaptic membranes of the cerebellar granule cells (CGCs) (Nusser et al., 1998) and dominate over other synaptic α subunits in mature rodent cerebellum and throughout the brain (Laurie et al., 1992; Wisden et al., 1992; Fritschy et al., 1994). Abundant expression of the α1 subunit suggests it as a crucial component of GABA$_A$-mediated neurotransmission in the brain. A number of studies have demonstrated involvement of α1 in mediation of sedative, amnesic, and anticonvulsive effects of a variety of pharmacological agents (Rudolph et al., 1999; Crestani et al., 2002; Kralic et al., 2002). It is of note that, with the exception of a slight handling tremor (Kralic et al., 2002, 2005), deletion of the α1 subunit gene produces no pronounced phenotype (Rudolph and Mohler,

2004; Vicini and Ortinski, 2004), implying unidentified compensatory mechanisms.

In an examination of possible synaptic sources of such compensation, we reported previously the impact of α1 deletion on the development of IPSCs in cerebellar slices and CGC cultures (Vicini et al., 2001; Ortinski et al., 2004) and suggested several compensatory mechanisms. In particular, as also evidenced by biochemical studies (Sur et al., 2001; Kralic et al., 2002), retention of α2/α3 subunits at synapses or their compensatory upregulation may take place in the α1$^{-/-}$ mice. Functionally, increased duration of synaptic events in the α1$^{-/-}$ mice may counterbalance their decrease in amplitude to maintain unperturbed levels of synaptic charge transfer (Ortinski et al., 2004).

A low concentration of GABA (Farrant and Nusser, 2005) continuously present in the extracellular space is another source of inhibition in the cerebellum and the brain. Ambient GABA concentration is likely established by GABA spilled over outside the synapse after vesicular release (Brickley et al., 1996; Wall and Usowicz, 1997; Rossi and Hamann, 1998), although other sources are possible (Semyanov et al., 2004; Farrant and Nusser, 2005). In CGCs, ambient GABA activates predominantly the high-affinity extrasynaptic receptors containing α6 and/or δ subunits (Rossi and Hamann, 1998; Hamann et al., 2002). Such

"tonic" inhibition was shown to be a powerful modulator of neuronal excitability (Hamann et al., 2002; Mitchell and Silver, 2003), and its behavioral importance has been a subject of keen interest in recent years (Semyanov et al., 2003; Hanchar et al., 2005; Maguire et al., 2005; Scimemi et al., 2005).

In the cerebellum of α1$^{-/-}$ mice, in which a major synaptic GABA$_A$ receptor subunit and >50% of the total GABA$_A$ receptors are lost (Kralic et al., 2002), the mild phenotype is remarkable and tonic GABA$_A$-mediated conductance presents an attractive target for compensatory action. There are two general mechanisms through which a tonic whole-cell conductance can be altered. One is through changes in expression level or biophysical properties of the receptors responsible for activating tonic conductance. The other one is through changes in extracellular GABA concentration. In this study, we report an increase of tonic GABA$_A$ receptor-mediated conductance in the CGCs in slices from α1$^{-/-}$ mice and identify reduction of GABA transporter (GAT) activity as the likely source of this change.

Materials and Methods

Mutant mice and genotyping. α1 subunit-deficient mice were produced at the University of Pittsburgh as described previously (Vicini et al., 2001) and shipped to Georgetown University for all experimental procedures. Heterozygous mice on a mixed genetic background (C57BL/6J, strain 129/Sv/SvJ, and FVB/N) (Vicini et al., 2001) were interbred to produce wild type (WT) (+/+), heterozygous (+/−), and homozygous (−/−) α1 mice. PCR was used to genotype mutant mice as described by Ortinski et al. (2004). Briefly, total genomic DNA was isolated at postnatal day 3 (P3) to P6 from tail snips, amplified with PCR, separated by electrophoresis, and visualized with ethidium bromide staining. Twenty-seven PCR cycles were run after initial denaturation at 95°C for 5 min. Each cycle consisted of denaturation at 95°C for 1 min, primer annealing at 57°C for 1.5 min, and primer elongation at 72°C for 2 min. A final elongation step was performed at 72°C for 3 min.

Western blot analysis and quantification. All Western blot procedures were done in triplicate for each genotype. Whole cerebella of +/+ and α1$^{-/-}$ P23 mice were homogenized in TEE buffer (in mM: 10 Tris-HCl, pH 7.4, 1 EDTA, and 1 EGTA). The homogenates were centrifuged at 30,000 × g_{max} at 4°C for 16 min to obtain the crude membrane fraction and resuspended in TEE buffer. Protein was determined with the Coomassie Plus Protein Assay (Pierce, Rockford, IL). After separation in a 7.5% polyacrylamide gel, proteins were transferred to polyvinylidene difluoride (PVDF) membranes and incubated at room temperature in TBST (20 mM Tris-HCl, pH 7.4, 140 mM NaCl, and 0.1% Tween 20) containing 5% nonfat dried milk for 20 min. The membranes were then incubated overnight at 4°C with affinity-purified rabbit antibodies directed against GAT-1 (1:500; Chemicon, Temecula, CA) or GAT-3 (1:1000; Alpha Diagnostic, San Antonio, TX). After four 5 min washes in TBST, the membranes were incubated with horseradish peroxidase-labeled antibody (1:5000; Amersham Biosciences, Piscataway, NJ) for 30 min at room temperature. The membranes were then washed with TBST once for 15 min and four times for 5 min, and protein bands were visualized on a photographic film with Super Signal West-Pico chemiluminescence reagents (Pierce). The integrated intensity of each band was calculated using computer-assisted densitometry with Intelligent Quantifier software (Bio Image Systems, Jackson, MI).

Cerebellar slices. P22–P25 mice were killed by decapitation in agreement with the guidelines of the Georgetown University Animal Care and Use Committee. Whole cerebella were dissociated from the cortex and placed in an ice-cold slicing solution containing the following (in mM): 85 NaCl, 2.5 KCl, 1 CaCl$_2$, 4 MgCl$_2$, 1 NaH$_2$PO$_4$, 25 NaHCO$_3$, 25 glucose, and 75 sucrose (all from Sigma, St. Louis, MO) (pH 7.4 when continuously bubbled with 95% O$_2$ and 5% CO$_2$). Sagittal cerebellar slices, 200 μm thick, were prepared using Vibratome 3000 Plus Sectioning System (Vibratome, St. Louis, MO) and incubated in the slicing solution at 34°C for 30 min before being transferred to the recording solution. Slices were viewed under an upright microscope (E600FN; Nikon, Tokyo, Japan)

equipped with Nomarski optics and an electrically insulated 60× water-immersion objective with a long working distance (2 mm) and high numerical aperture (1.0).

[³H]GABA uptake. Cerebellar slices prepared as above were incubated in extracellular recording solution containing 400 nM [³H]GABA (NEN, Boston, MA) for 2 min at either 37°C (total [³H]GABA uptake) or 0°C (nonspecific [³H]GABA uptake). To terminate the assay, the slices were then washed three times with 0°C recording solution. NaOH (0.1N) was added, and samples were counted for radioactivity in a scintillation counter. Specific [³H]GABA uptake was determined by subtracting the nonspecific from the total [³H]GABA uptake and normalized to the total protein concentration.

Biotinylation. EZ-Link Sulfo-NHS-SS-Biotin (Pierce) was used to surface label proteins in cerebellar slices prepared as above. Slices were incubated with 1 mg/ml Sulfo-NHS-SS-Biotin in the recording solution at 4°C with gentle rocking for 1 h. Slices were then washed three times with ice-cold TBS (50 mM Tris-HCl and 150 mM NaCl) to remove and block unreacted Sulfo-NHS-SS-Biotin. TBS from each pool of cerebellar slices was removed, and the pelleted slices were placed in TEE. Each pool was sonicated with a Tekmar (Cincinnati, OH) TM-50 at a setting of 60 for 10 s in 5 ml of TEE. After centrifugation at 4°C for 16 min at 32,000 × g_{max}, samples were resuspended into 0.2 ml of TEE and stored at −70°C. Samples were placed in 1% deoxycholate and 50 mM Tris-HCl, pH 9, sonicated briefly, and incubated at 37°C for 30 min, mixing every 5 min to allow for solubilization of membrane proteins. Samples were then centrifuged at 4°C for 30 min at 32,000 × g_{max}. Supernatants were removed and kept on ice. Supernatant, 150 μl of each, was added to 25 μl of settled Neutravidin beads and incubated for 1 h at 4°C with rotation. Proteins were separated, transferred to PVDF, and probed with rabbit antibodies to GAT-1 (0.2 μg/ml; Chemicon) or GABA α6 subunit (1:1000; kind gift from Dr. Angel De Blas, University of Connecticut, Storrs, CT) as in Western blot analysis above. Primary antibodies were removed, and immunoblots were washed with TBST, incubated with 1:20,000 of HRP-conjugated donkey anti-rabbit IgG antibodies (Amersham Biosciences) for 30 min, and then washed with TBST. Immunoblot visualization and analysis was performed as for Western blot above. Percentage surface expression was determined by the amount found in the Neutravidin pellet divided by the sum of the Neutravidin pellet and supernatant.

Electrophysiology. Recordings were done in cerebellar granule cells in slices from +/+ and α1$^{-/-}$ littermates in parallel on the same day whenever possible. All recordings were performed at room temperature (24–26°C). Continuously perfused extracellular solution, unless otherwise indicated, contained the following (in mM): 120 NaCl, 3.1 KCl, 2 CaCl$_2$, 1 MgCl$_2$, 1 KH$_2$PO$_4$, 25 NaHCO$_3$, 2.5 glucose, and 30 sucrose (all from Sigma) (pH 7.4 when bubbled with 95% O$_2$ and 5% CO$_2$). Recording electrodes were pulled in two stages on a vertical pipette puller from borosilicate glass capillaries (Wiretrol II; Drummond, Broomall, PA) and filled with recording solution containing the following (in mM): 145 KCl or 135 CsCl, 10 HEPES, 5 ATP-Mg, 0.2 GTP-Na, and 10 BAPTA, adjusted to pH 7.2 with KOH. There were no differences in tonic current size or variability between CsCl and KCl experiments for either genotype, and the reported values for these measures represent pooled data from both CsCl and KCl experiments. For some experiments, NaCl (5 or 20 mM) and GABA (1 or 20 mM) were added to the intracellular recording solution to induce GABA transporter reversal (Wu et al., 2003); KCl concentration was then appropriately reduced to maintain osmolarity. Pipette resistance was 7–10 MΩ. Whole-cell voltage-clamp recordings were made at −60 mV with an Axopatch-1D amplifier (Molecular Devices, Palo Alto, CA), and access resistance was monitored throughout the recordings. Resting membrane potential was within the expected range (−65 to −75 mV) and was not different between genotypes ($p >$ 0.46). Membrane capacitance was calculated from a transient current response to a hyperpolarizing 10 mV pulse with the following equation: $C_m = \tau/R_s$, where τ is the time constant of the exponentially decaying capacitive current, and R_s is series resistance. Single-channel recordings were made from excised outside-out patches held at −100 mV to increase detection of small-amplitude events. Currents were filtered at 2 kHz with a low-pass Bessel filter and digitized at 5–10 kHz (for whole cells) and 20 kHz (for single channels) using a personal computer

equipped with Digidata 1322A data acquisition board and pClamp9 software (both from Molecular Devices). Stock solutions of bicuculline methobromide (BIC), NO711 (1-[2([(diphenylmethylene)imino]oxy)-ethyl]-1,2,5,6-tetrahydro-3-pyridinecarboxylic acid hydrochloride), gabazine (SR95531) [2-(3-carboxypropyl)-3-amino-6-(4-methoxy-phenyl)pyridazinium bromide], tetrodotoxin (TTX), 4,5,6,7-tetrahydroisoxazolo[5,4-c]pyridin-3-ol (THIP), and GABA (all from Sigma) were prepared in water and diluted to the desired concentration in extracellular medium. All drugs were locally applied through a Y tube (Murase et al., 1989) modified for optimal solution exchange in brain slices (Hevers and Luddens, 2002).
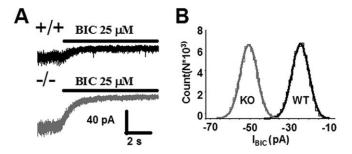
Data analysis. Tonic current was measured as the difference in the mean baseline current devoid of synaptic events during and before application of BIC (25 μM). Baseline current was computed from a minimum of 3 s of continuous recording. Recordings with unstable baseline (>10% difference from the mean baseline current) were not included in the analyses. Trace segments without synaptic current were selected. The PSCs are very infrequent in the knock-out, and in the WT the PSC frequency is low enough to consistently allow the selection of synaptic current-free segments of 3 s or more. Current density was computed as the ratio of I/C_m. Dose–response curves were fitted using Origin (Microcal Software, Northampton, MA) with the following logistic function: $I_{peak} = I_{min} + (I_{max} - I_{min}/1 + ([Drug]^{slope}/EC_{50}))$, where I_{min} and I_{max} are minimal and maximal evoked currents, [Drug] is GABA or THIP concentration, and slope is slope of the curve. Events for single-channel dwell time analyses were collected using half-amplitude threshold detection method built into Clampfit 9 software (Molecular Devices). A minimum of 1000 events were collected for all conditions. Superimposed openings were excluded. Logarithmic open interval distributions were binned and fitted with a sum of three logarithmic exponential probability density functions using the maximum likelihood method after taking the square root of the bin counts to improve statistical scatter of the data (Sigworth and Sine, 1987). Instantaneous frequency of single-channel openings was calculated as the inverse of the time elapsed between the start of current and the start of last event averaged across all registered events. Mean unitary current was determined from the fits of amplitude distributions with Gaussian components. Single-channel chord conductance was determined from the unitary current and the Cl^- driving force. Alternatively, single-channel slope conductance was estimated from the linear fit of the I–V relationship. Only the openings to the main conductance level were considered for the I–V fit. All single-channel data analyses were performed with Clampfit 9 software. Statistical comparisons were done using a two-tailed Student's *t* test assuming homogeneity of variances of the samples as verified by *F* test. All data are expressed as mean ± SEM, unless otherwise indicated.
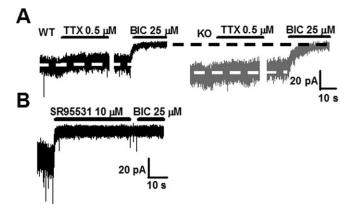
Results

Tonic GABA_A-mediated current

Whole-cell tonic current was measured after application of BIC (25 μM) as described in Materials and Methods. Measurements were done in mice from eight different litters. Tonic current in cerebellar granule neurons in slices from α1 −/− mice was 62% larger than tonic current measured in +/+ CGCs (−/−, 39 ± 3 pA, n = 32; +/+, 24.1 ± 3 pA, n = 31; p < 0.01) (Fig. 1). The variance of the baseline devoid of synaptic events (in the absence of BIC) was larger in the α1 −/− CGCs (34.7 ± 4.4 pA^2) and significantly different from the +/+ (23.3 ± 2.7 pA^2; p = 0.03). The difference in the coefficient of variance of the baseline current in the absence of BIC was not significant (−/−, 14 ± 2%; +/+, 14 ± 3%; p = 0.81). Granule cells in both genotypes were similar in size as assessed by visual inspection and capacitance measurements (−/−, 4.2 ± 0.2 pF, n = 12; +/+, 4.4 ± 0.3 pF, n = 12; p > 0.65).

Bicuculline is known to block also nicotinic ACh receptors (Rossi et al., 2003). To ensure that tonic current was mediated by GABA_A receptors in both genotypes, another, more specific GABA_A antagonist, gabazine (SR95531, 10 μM) was applied be-

Figure 1. Larger tonic GABA_A receptor-mediated current in CGCs of α1 −/− mice. *A*, Representative current traces from cerebellar granule cells in brain slices of wild-type (+/+, top) and α1 knock-out (−/−, bottom) mice. Application of the competitive GABA_A antagonist BIC (25 μM) reveals a tonic conductance. *B*, Amplitude distributions of current traces in *A*. Distributions were drawn from current segments immediately preceding BIC application. Mean baseline current during application of BIC (25 μM) was adjusted to 0. The average values of tonic current, normalized to the cell capacitance were as follows: 6 ± 0.75 pA/pF, n = 31 for +/+; 9.75 ± 0.75 pA/pF, n = 32 for α1 −/−; p < 0.02. Tonic current was calculated as described in Materials and Methods. Data are derived from >15 mice in eight litters. For values of variance and coefficient of variation of the baseline noise, see Results.

Figure 2. Increased tonic current in the α1 −/− CGCs is not accounted for by increased action potential-dependent vesicular release or nonspecificity of BIC. *A*, Representative traces showing a slight inhibition of tonic current by TTX (0.5 μM) in +/+ (left, black) and α1 −/− (right, gray) slices. The full extent of tonic conductance in these cells can be seen during application of BIC (25 μM). White dotted lines are centered at the mean baseline current in the absence of TTX; a small inward current immediately preceding TTX application is a delivery method artifact. A spontaneous IPSC can be seen in the +/+ trace; in the α1 −/−, spontaneous IPSCs are observed but at much lower than +/+ frequency (unpublished observation). The breaks between TTX and BIC applications are not drawn to scale; total duration of TTX application for the WT trace in this panel was 44 s and for the KO trace was 30 s. There were no differences in TTX effect on tonic current between genotypes: +/+, 3.1 ± 0.7 pA, n = 25; −/−, 3.5 ± 1.4 pA, n = 12; p = 0.75. *B*, Application of the specific GABA_A antagonist SR95531 (10 μM) completely blocks tonic current without additional inhibition by BIC as illustrated in this P25 +/+ trace. Not shown is application of SR95531 after BIC without a change of baseline current. Similar results were observed in two other +/+ and three α1 −/− cells.

fore and after application of BIC in a separate experiment. No changes in baseline inhibition were observed between the two antagonists (Fig. 2B), indicating that tonic non-GABA_A-mediated conductances do not appreciably contribute to bicuculline-sensitive tonic current in our conditions. Furthermore, in 10 +/+ and 10 −/− cells, K^+ conductance was blocked by substituting CsCl for KCl in the intracellular solution. These experiments revealed no differences in tonic current size between the CsCl-containing (+/+, 20.3 ± 2.6 pA, n = 10; −/−, 35.6 ± 3 pA, n = 10; p < 0.01) and KCl-containing (+/+, 25.9 ± 4.2 pA, n = 21; −/−, 39.5 ± 4.6 pA, n = 22; p = 0.03) solutions for neither +/+ (p = 0.35) nor −/− (p = 0.4) cells.

Because neurotransmitter spillover after vesicular release is

thought to be a major source of ambient GABA, we looked at whether action potential-dependent vesicular release is different between the +/+ and the α1 $^{-/-}$ mice. Consistent with the reports of action potential-independent vesicular release in late postnatal development in rats (Wall and Usowicz, 1997; Hamann et al., 2002), application of TTX (0.5 μM) had only minor effects on tonic current in both genotypes and was not significantly different between them (Fig. 2A).

Role of α6 and δ subunit-containing receptors

A change in number of extrasynaptic receptors is one possible source of the tonic GABA$_A$ current increase in the α1 $^{-/-}$ mice. In the mouse cerebellum, these receptors contain α6 and δ subunits, and several lines of evidence suggest their colocalization in the same protein (Jones et al., 1997; Nusser et al., 1998).

To uncover a possible upregulation of the α6 and δ subunit-containing GABA$_A$ receptors, we recorded whole-cell responses to a range of concentrations of GABA$_A$ partial agonist THIP and normalized them in each cell to a response evoked by saturating [GABA] (1 mM) (Fig. 3). THIP has been used at low concentrations to activate δ subunit-containing extrasynaptic receptors in the thalamus (Belelli et al., 2005; Cope et al., 2005). Although it is not a subunit-selective GABA$_A$ agonist, THIP has increased efficacy at the α4 and δ subunit-containing GABA$_A$ receptors and comparable with GABA potency and efficacy at the α6 subunit-containing receptors (Ebert et al., 1997; Brown et al., 2002). At high concentrations, THIP is expected to behave as a nonselective GABA$_A$ agonist, and the fitted dose–response curves indicated a loss of low-affinity THIP-sensitive receptors in the α1 $^{-/-}$ cells, consistent with the lack of the α1 subunit (Fig. 3B). Because α1 subunits are unavailable for activation and currents evoked by saturating GABA in the α1 $^{-/-}$ were only 32% of those in the +/+ CGCs (Fig. 3A), the contribution of α6 and δ subunit-containing receptors to the total GABA$_A$-mediated current is significantly larger in the α1 $^{-/-}$ mice (Fig. 3B). However, at low doses of THIP (0.5 and 5 μM), an average whole-cell response was not significantly different between genotypes, although a trend toward smaller responses in the α1 $^{-/-}$ group increased with increasing THIP concentrations (Fig. 3C). Therefore, confirming a recent biochemical report (Ogris et al., 2006), we observe no increase of functional, low-[THIP]-sensitive α6 and δ subunit-containing GABA$_A$ receptors in the α1 $^{-/-}$ CGCs.

As additional confirmation of these observations, we exploited the characteristic high affinity of extrasynaptic α6 and δ subunit-containing receptors for GABA (Saxena and Macdonald, 1994, 1996; Ducic et al., 1995) to compare the abundance of these subunits in the α1 $^{-/-}$ with the +/+ neurons. Measurements of whole-cell currents elicited by low concentrations of GABA revealed no significant difference between genotypes (Fig. 3D), although, once again, contribution of the high-affinity GABA$_A$ receptors to total GABA conductance was significantly larger in the α1 $^{-/-}$ group because of, as with THIP, a dramatic reduction of response to saturating GABA (Fig. 3A,E).

Single-channel properties of extrasynaptic receptors

We then explored the possibility that a change of biophysical properties of extrasynaptic GABA$_A$ receptors might account for the increase of tonic current observed in CGCs of the α1 $^{-/-}$ mice. Recording GABA$_A$ receptor currents in outside-out patches excised from CGCs revealed an abundance of brief single-channel openings in the α1 $^{-/-}$ group (Fig. 4A,B). In the presence of 50 μM GABA, the mean single-channel open time was 46% shorter in the α1 $^{-/-}$ than in the +/+ patches, a difference
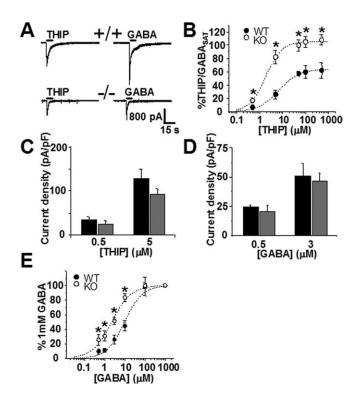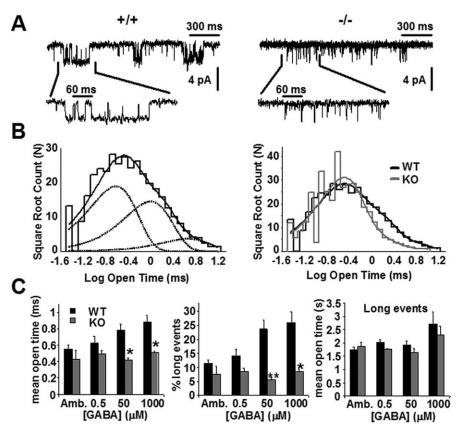

Figure 3. Sensitivity of GABA$_A$ receptors to activation by THIP (Gaboxadol) and low GABA concentrations in CGCs lacking the α1 subunit. **A**, Whole-cell responses of granule cells in cerebellar slices from +/+ (top) and α1 $^{-/-}$ (bottom) mice to applications of THIP (50 μM) and GABA (1 mM). Notice a decrease in both THIP- and GABA-activated currents in the α1 $^{-/-}$. Applying a saturating concentration of GABA (1 mM) allowed for an estimate of the total functional GABA$_A$ receptors in the +/+ and α1 $^{-/-}$ groups. Average current densities calculated from responses to 1 mM GABA were as follows: 382 ± 62 pA/pF, n = 10 for +/+; 123 ± 26 pA/pF, n = 10 for −/−; p < 0.01. **B**, Whole-cell THIP dose–response normalized to currents elicited by saturating GABA (1 mM; GABA$_{SAT}$). Response at each concentration was normalized to GABA applied to the same cell. Notice the difference in maxima (+/+, 67 ± 5%; −/−, 105 ± 8%). EC$_{50}$ values are 6.8 ± 0.9 μM for +/+ (n_H = 0.9) and 1.3 ± 0.9 μM for α1 $^{-/-}$ (n_H = 0.95). Currents from 5–10 cells were recorded at each concentration. *p < 0.05. **C**, Whole-cell current density evoked by the two lowest THIP concentrations. The difference between THIP-evoked currents in the +/+ (black; 0.5 μM, 36 ± 5 pA/pF, n = 8; 5 μM, 128 ± 22 pA/pF, n = 6) compared with the α1 $^{-/-}$ (gray; 0.5 μM, 25 ± 6 pA/pF, n = 7; 5 μM, 93 ± 12 pA/pF, n = 12) becomes larger at higher [THIP]. **D**, Low concentrations of GABA elicit similar whole-cell responses in CGCs of +/+ (black; 0.5 μM, 24 ± 2 pA/pF, n = 8; 3 μM, 51 ± 11 pA/pF, n = 12) and the α1 $^{-/-}$ (gray; 0.5 μM, 21 ± 5 pA/pF, n = 6; 3 μM, 47 ± 7 pA/pF, n = 16) mice (p > 0.4 for both concentrations). **E**, GABA dose–response curves in +/+ and α1 $^{-/-}$ cells normalized to currents evoked by saturating GABA (1 mM). Response at each concentration was normalized to GABA applied to the same cell. Currents from 6–16 cells were measured for each concentration point. EC$_{50}$ values determined from fitted curves are 10 ± 1.2 μM for +/+ (n_H = 1.1) and 1.3 ± 0.9 μM for α1 $^{-/-}$ (n_H = 0.95). *p < 0.05.

significant at p = 0.01 (Fig. 4C, left). Across four GABA concentrations (endogenous GABA and three exogenously applied concentrations), the mean single-channel open time was 32% shorter in the α1 $^{-/-}$ patches (Fig. 4C, left). Short mean open times observed here are consistent with the kinetic behavior of the high-affinity α6 and δ subunit-containing receptors (Fisher and Macdonald, 1997; Fisher 2004).

For purposes of additional analysis, we defined long-lived open intervals as those lasting >1 ms (based loosely on the point of divergence of +/+ and α1 $^{-/-}$ open interval distributions as in Fig. 4B). Increasing GABA concentrations activated increasingly more long-lived states in patches from the +/+ but not the α1 $^{-/-}$ cells (Fig. 4C, middle), likely indicative of a progressive recruitment of the low-affinity (α1-containing) receptors in the wild type. This suggestion, however, must be interpreted with

Figure 4. Single-channel recordings reveal long-lived open states in patches excised from CGCs of +/+ but not α1 $^{-/-}$ cells. **A**, Examples of single-channel traces from CGC patches of +/+ (left) and α1 $^{-/-}$ (right) mice at P23 during an application of 50 μM GABA. Recordings were obtained in isotonic Cl$^-$ with V_h of −100 mV. Notice short open intervals in the +/+ patch. Traces filtered at 1000 Hz for display only. **B**, Left, Binned logarithmic distribution of open intervals during continuous application of 50 μM GABA for the +/+ patch illustrated in **A**, fitted with a sum of three exponential components. Right, A scaled overlay of this distribution (black) with an open time distribution for the α1 $^{-/-}$ patch in **A** (gray) illustrates similar distributions of short open intervals but a greater proportion of longer open intervals for channels in +/+ patches. The time constants (and relative areas) of the components are as follows: +/+, 0.36 (0.51), 1.52 (0.39), and 7.1 (0.1); −/−, 0.27 (0.79), 1.02 (0.17), and 5.73 (0.03). The mean open times across four +/+ and three α1 $^{-/-}$ patches in the presence of 50 μM GABA are 0.78 ± 0.09 and 0.42 ± 0.02 ms, respectively ($p = 0.01$). **C**, Sensitivity of short and long open intervals in patches from +/+ (black bars) and α1 $^{-/-}$ (gray bars) mice to increasing GABA concentrations. Amb, Open intervals collected in the presence of endogenous (ambient) and absence of exogenous GABA. Left, A histogram of mean open intervals of GABA$_A$ channels in +/+ and α1 $^{-/-}$ patches at different GABA concentrations ($n = 3$ – 4 patches in each condition; *$p = 0.01$). Middle, A histogram of the number of long open intervals (≥1 ms) at different GABA concentrations in patches from +/+ and α1 $^{-/-}$ cells. Long openings are expressed as a percentage of all events within the same time interval (*$p = 0.01$, **$p < 0.01$). Right, A histogram of mean open times of long (≥1 ms) open intervals. Differences between the +/+ and the −/− patches are not statistically significant ($p > 0.08$ at 0.5 μM and $p > 0.48$ at all other concentrations).

caution in view of a nonzero probability of observing α6 and δ subunit-containing receptors in a long-lived open state (Fisher and Macdonald, 1997; Fisher, 2004). The fact that a small portion (<10%) of all open intervals in the α1 $^{-/-}$ cells were long (Fig. 4C, middle) implicates α6-, δ-, or α2/3-containing GABA$_A$ receptors (see Discussion). The number of long-lived open intervals did not change with increasing GABA concentrations in the α1 $^{-/-}$ cells but increased more than twofold from lowest to highest GABA concentration in the +/+ (Fig. 4C, middle) cells. No significant differences in the duration of long-lived open states were detected between the α1 $^{-/-}$ and the +/+ groups (Fig. 4C, right).

No differences between genotypes were found in single-channel conductance (in the presence of 50 μM GABA, +/+, 24 ± 2 pS, $n = 3$; −/−, 22 ± 0.6 pS, $n = 3$; $p = 0.38$). The overall frequency of single-channel openings was likewise not significantly different between genotypes whether when measured as
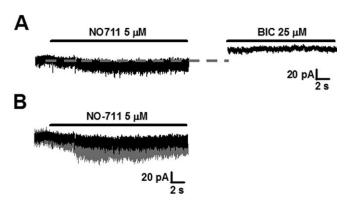
events per second (in 500 nM GABA, +/+, 92 ± 42; −/−, 131 ± 76, $p = 0.59$; in 50 μM GABA, +/+, 179 ± 116; −/−, 203 ± 153, $p = 0.82$) or instantaneous frequency (in 500 nM GABA, +/+, 738 ± 207; −/−, 481 ± 101, $p = 0.08$; in 50 μM GABA, +/+, 705 ± 119; −/−, 580 ± 158, $p = 0.28$). Lack of frequency differences with high [GABA] may prove intriguing provided the caveats of frequency estimation are considered (see Discussion).

Together with the mean open time analyses and results of whole-cell current measurements, these data bring additional support to the hypothesis that compensatory upregulation of high-affinity extrasynaptic α6 and δ subunit-containing GABA$_A$ receptors or compensatory changes in single-channel properties are not responsible for tonic current increase in the α1 $^{-/-}$ CGCs.
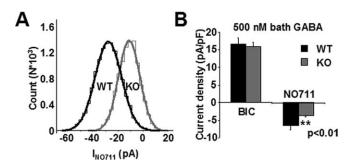
Role of uptake transporters

The active role of uptake transporters in regulation of extracellular neurotransmitter concentration has been emphasized in a number of recent publications (Semyanov et al., 2003; Chiu et al., 2005; Wadiche and Jahr, 2005). In the rodent cerebellum, GABA uptake is mediated by GAT-1 and GAT-3. GAT-1 expression is mostly localized to neurons, whereas GAT-3 is preferentially expressed in the glia (Itouji et al., 1996; Pow et al., 2005). NO711-sensitive GAT-1 fraction accounts for up to 85% of all GABA transport in whole-cerebellum preparations (Chiu et al., 2005). If ambient GABA concentration is higher in the α1 $^{-/-}$ than in the +/+, then more GATs should be recruited at any given time in slices from the α1 $^{-/-}$ mice, assuming that transporters work in the forward direction transporting GABA into the cell and are not already saturated by a lower-than-ambient GABA.

To assess transporter activity in the two genotypes, we performed CGC recordings in the presence of the GAT-1-specific blocker NO711 (5 μM). Application of NO711 elicited an inward current, reflecting accumulation of GABA in the extracellular space; this current was completely blocked by 25 μM BIC (Fig. 5A). NO711-evoked currents were significantly larger in CGCs from the α1 $^{-/-}$ mice (14.9 ± 2.1 pA; $n = 20$) than from the +/+ mice (8.4 ± 1.5 pA; $n = 31$; $p = 0.01$) (Fig. 5B). We also investigated the effect of GAT-1 blockade under conditions when reversed transport was induced in the +/+ and α1 $^{-/-}$ CGCs by increasing intracellular NaCl and GABA concentrations to 5 mM NaCl and 1 mM GABA in one experiment and to 20 mM both NaCl and GABA in another (and reducing intracellular KCl to maintain osmolarity; see Materials and Methods) as described by Wu et al. (2003). Under these conditions, application of NO711 still evoked an inward current, albeit of slightly smaller magnitude (on average, ∼2 pA smaller than under normal conditions in the same genotype; data not shown). We conclude that

Figure 5. Differences in endogenous extracellular GABA concentration enhance GABA transporter activity in the $\alpha 1^{-/-}$ mice. *A*, A representative trace from a CGC in a P23 $+/+$ slice. Blocking GABA uptake with the GAT-1 inhibitor NO711 results in accumulation of GABA in the extracellular space and activation of tonic BIC-sensitive conductance. The gray dotted line is centered at the mean baseline current in the absence of NO711. *B*, An overlay of $+/+$ (black) and $\alpha 1^{-/-}$ (gray) traces illustrating the effect of GABA uptake inhibition in the two genotypes. NO711-evoked currents were on average 77% larger in the $\alpha 1^{-/-}$ compared with $+/+$ CGCs (for current values, see Results).
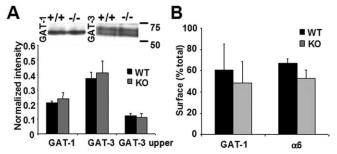

Figure 6. BIC-sensitive tonic current and NO711-evoked currents measured in CGCs from $+/+$ and $\alpha 1^{-/-}$ slices maintained in extracellular solution containing 500 nM GABA. *A*, Current amplitude distributions of 2.5 s segments of current traces devoid of synaptic currents from one $+/+$ (black fit) and one $\alpha 1^{-/-}$ (gray fit) CGC during application of NO711 (5 μM). The mean baseline current immediately preceding NO711 application was adjusted to 0 in both cases. Gaussian fits of these distributions give mean peak amplitude values of -27.7 ± 0.06 pA for $+/+$ and -11 ± 0.13 pA for $\alpha 1^{-/-}$. *B*, No significant differences between genotypes were observed during application of 25 μM BIC. Application of NO711 elicited an average of 86% larger ($p < 0.01$) currents in the $+/+$ than in the $\alpha 1^{-/-}$ neurons (for current values, see Results).

GAT-1 located on the recorded CGCs contribute only minimally to the overall GAT-1 activity. Therefore, it is unlikely that the results of NO711 application in the recordings with normal intracellular solution are an artifact of replacing endogenous intracellular milieu with intracellular recording solution.

We next asked whether increased extracellular GABA concentration in the CGCs from $\alpha 1^{-/-}$ was a result of lower GAT-1 activity in the cerebellum of these mice. Because GAT-1 activity depends on extracellular GABA concentration, we recorded NO711-evoked tonic currents from $+/+$ and $\alpha 1^{-/-}$ slices continuously perfused with extracellular solution containing 500 nM GABA. Wild-type and $\alpha 1^{-/-}$ slices were kept in the same recording chamber for equal periods of time, and recordings were done alternately from $+/+$ and $\alpha 1^{-/-}$ cells. With 500 nM GABA in the bath, application of NO711 elicited significantly larger inward current in $+/+$ CGCs (26.5 ± 4.5 pA; $n = 11$) than in the $\alpha 1^{-/-}$ CGCs (14.2 ± 1.7 pA; $n = 14$; $p < 0.01$) (Fig. 6 *A*,*B*).

Additionally, no differences in tonic bicuculline-sensitive current were seen in the presence of 500 nM bath GABA ($+/+$,

Figure 7. GAT-1 and GAT-3 protein expression. *A*, Top, Western blot samples of $+/+$ and $\alpha 1^{-/-}$ staining with antibodies directed against GAT-1 (67 kDa) and GAT-3 (71 kDa). GAT-3 staining revealed a doublet with no band intensity differences between the entire band or the individual upper and lower bands. Bottom, A histogram of average normalized band intensity from three $+/+$ and three $\alpha 1^{-/-}$ samples. GAT-3 upper, Upper band of the GAT-3 doublet. *B*, Comparison of the surface expression of GAT-1 and GABA$_A$ α6 subunit in mouse cerebellar slices in $+/+$ (GAT-1, $61 \pm 24\%$; α6, $67 \pm 4\%$; $n = 3$) and $\alpha 1^{-/-}$ (GAT-1, $48 \pm 20\%$; α6, $53 \pm 7\%$; $n = 4$). The values are not significantly different ($p = 0.66$ for GAT-1; $p = 0.15$ for α6). Percentage surface expression was determined as described in Materials and Methods.

66.6 ± 7.4 pA, $n = 14$; $-/-$, 63.2 ± 3.2 pA, $n = 23$; $p = 0.64$) (Fig. 6 *B*). These results support our conclusion that tonic GABA$_A$ current increase in CGCs from $\alpha 1^{-/-}$ mice is mediated by increased extracellular GABA concentration and suggest that decreased GAT-1 activity in the $\alpha 1^{-/-}$ may underlie such increase in concentration.

We investigated, therefore, whether a decrease in GAT-1 protein expression is responsible for decreased GAT-1 activity and probed also the expression levels of GAT-3 protein. As shown in Figure 7*A*, immunoblotting of the membrane-bound GAT-1 and GAT-3 proteins revealed no differences in normalized band intensity for either protein between three $+/+$ (GAT-1, 0.21 ± 0.01; GAT-3, 0.37 ± 0.05) and three $\alpha 1^{-/-}$ (GAT-1, 0.24 ± 0.04, $p = 0.42$; GAT-3, 0.41 ± 0.08, $p = 0.62$) mice. Given that Western blot resolution is limited to an approximately twofold change of labeled protein and reflects the protein from the whole cerebellum, it is possible that a smaller or a very local change of GAT-1 or GAT-3 protein expression escaped detection by this method. Alternatively, GAT-1 activity difference between genotypes is a result of a difference in the efficiency of transport but not the number of GAT-1 proteins (see Discussion). Thus, we compared the efficiency of GABA transport in cerebellar slices from $\alpha 1^{-/-}$ and $+/+$ mice by [^{3}H]GABA uptake assay. Slices from $\alpha 1^{-/-}$ incorporated an average of 20% less radioactive GABA via uptake mechanisms than their $+/+$ counterparts (16.3 ± 1.1 pmol/mg protein for $+/+$, $n = 3$; 11.6 ± 1.2 pmol/mg protein for $\alpha 1^{-/-}$, $n = 3$; $p < 0.05$), indicating impaired transport and providing a physiological basis for increased tonic GABA current in cerebellar granule cells of these mice.

α6 and GAT-1 surface expression

Our results argued against both an increased expression of α6 and δ subunit-containing GABA$_A$ receptors and decreased expression of GABA uptake transporters, the most obvious possible mediators of tonic GABA$_A$ current increase. In an effort to confirm these conclusions, we looked at the expression of α6 subunit and GAT-1 proteins on the cell surface by use of a biotinylation agent. Biotinylation assays revealed no difference in cell surface expression of either of the two proteins between the two genotypes (Fig. 7*B*). Extending the Western blot analysis, these results further indicate that deletion of α1 subunit did not affect the recycling

rate of GAT-1 that could potentially lead to a change in surface expression of this protein in $\alpha1^{-/-}$ cells.

Discussion

Our first finding is that CGCs in mice with targeted deletion of the GABA$_A$ receptor α1 subunit gene manifest an increase of tonic GABA$_A$ receptor-mediated current. Such increase is potentially capable of compensating for the loss of phasic inhibitory drive to these cells, establishing an intriguing "balancing act" between synaptic and tonic forms of GABA$_A$-mediated inhibition. It must, however, be remembered that other regulatory mechanisms are activated after the disruption of the α1 gene (Vicini and Ortinski, 2004). These mechanisms may extend beyond the GABAergic system and beyond neurotransmitter signaling systems (Heinen et al., 2003; Reynolds et al., 2003). Related to tonic current is a study showing a K$^+$ conductance increase in CGCs of mice lacking the α6 subunit of the GABA$_A$ receptor (Brickley et al., 2001). Other systems notwithstanding, a 62% increase of tonic GABA$_A$-mediated inhibition that we observe, compounded with compensatory changes of synaptic currents (Vicini et al., 2001; Ortinski et al., 2004), is likely to play a major role in regulating neuronal excitability in these mice.

Multiple sources can lead to an increase of tonic current. Increase in expression of extrasynaptic high-affinity receptors is one, especially in light of evidence for coordinated expression of the α1, α6, β2, and γ2 genes (Uusi-Oukari et al., 2000). Biochemical studies, however, conclude that upregulation of α6 and δ subunit-containing GABA$_A$ receptors is absent in the $\alpha1^{-/-}$ mice, despite the increased levels of α6 protein (Ogris et al., 2006). Similarly, our biotinylation results indicate no change of α6 subunit expression on the cell surface. It is difficult to estimate the functional impact of these observations because the $\alpha1^{-/-}$ mice display a downregulation of β2/3 and γ2 subunit proteins, and this is often not paralleled by the corresponding mRNA level changes (Sur et al., 2001; Kralic et al., 2006; Ogris et al., 2006). Addressing the lack of functional data, our whole-cell recordings find no evidence of an increase in high-affinity, α6- and δ-containing GABA$_A$ receptors, despite the dramatic reduction of the total number of GABA$_A$ receptors activated by saturating [GABA]. This argues for independent regulation of expression of α1- versus α6- and δ-containing GABA$_A$ receptors in this knock-out model.

An increase of action potential-dependent vesicular GABA release is a possible source of increased ambient GABA. In our conditions, TTX blocked only a minor portion of the tonic current. The relative insensitivity of tonic current to TTX blockade has been reported in CGCs of rats of comparable age (Wall and Usowicz, 1997; Hamann et al., 2002; Wall 2005), although at least one report argues against such insensitivity in mice (Brickley et al., 2003). The issue could be related to the viability and/or activity of Golgi cells in different slice preparations. We observed no difference in the ability of TTX to block tonic GABA current in the CGCs of +/+ and $\alpha1^{-/-}$ mice. Rossi et al. (2003), however, reported activation of tonic current by action potential-independent nonvesicular release in rat CGCs. Future studies may elaborate on this alternative by recording from slices incubated with tetanus or botulinum toxins.

A difference in biophysical properties of single extrasynaptic GABA$_A$ receptor channels could underlie an increase in tonic current. GABA$_A$ receptor kinetics are susceptible to modulation by a variety of factors, including protein kinases (Nusser et al., 1999; Hinkle and Macdonald, 2003; Jovanovic et al., 2004), extracellular pH (Mozrzymas et al., 2003), and membrane voltage

(Pytel et al., 2005). We observed no differences between genotypes in single-channel conductance or frequency of openings across several GABA concentrations. Some caution is, however, required with interpretation of the frequency data considering the difficulty of controlling for equal number of channels in the excised patches.

The mean channel open time was invariably shorter in the $\alpha1^{-/-}$ cells and consistent with the kinetic behavior of α6 and δ subunit-containing receptors (Fisher and Macdonald, 1997; Fisher, 2004). Outside-out patches pulled from CGCs contain mostly extrasynaptic membranes (Nusser et al., 1998). Despite this, a small fraction of commonly synaptic α1β2/3/γ2 GABA$_A$ receptors can be identified on granule cell soma (Nusser et al., 1998). If α2/3 subunit-containing receptors, which are partially retained at mature synapses of $\alpha1^{-/-}$ mice (Vicini et al., 2001; Ortinski et al., 2004), are also delivered to somatic locations, they will have influenced our single-channel responses in the $\alpha1^{-/-}$ cells. Relative to α6- and δ-containing receptors, α2/3-containing receptors have lower affinity to GABA and enter long-lived open states (Gingrich et al., 1995; Saxena and Macdonald, 1996; Lavoie et al., 1997). Indeed, we observed a small fraction ($<$10%) of long-lived open states among the majority of short openings in patches from the $\alpha1^{-/-}$ CGCs. The fraction of these openings to the total number of events, however, did not increase with increasing GABA concentrations, as could be expected from an increasing recruitment of the low-affinity receptors and as was observed in patches from +/+ CGCs. Thus, long-lived open intervals in the +/+ likely represent a mixed response of the low-affinity α1-containing receptors and the high-affinity α6 and δ subunit-containing receptors, because α6- and δ-containing receptors are capable of entering such long-lived states with a low probability (Fisher and Macdonald, 1997; Fisher, 2004).

The absence of extrasynaptic receptor upregulation, shorter open time intervals, and comparable frequency of openings of channels in patches excised from $\alpha1^{-/-}$ CGCs suggest that an increase in extracellular GABA concentration is responsible for tonic current increase in these mice. Adding 500 nM GABA to the extracellular solution, in fact, eliminated the differences in tonic current between the +/+ and the $\alpha1^{-/-}$ CGCs. Moreover, recordings done under these conditions revealed a significantly smaller level of GAT-1 activity in the $\alpha1^{-/-}$ CGCs. Biochemical experiments with [^{3}H]GABA provided additional evidence of reduced transporter activity in the $\alpha1^{-/-}$ mice. Other conditions being equal, a reduction of uptake activity increases extracellular [GABA] and tonic GABA$_A$ current, as demonstrated in transgenic mice lacking GAT-1 (Chiu et al., 2005). One must be careful, nevertheless, about concluding that decreased GAT uptake precedes and causes the increase of ambient GABA concentration in the $\alpha1^{-/-}$ model. Given the evidence of plasticity of GAT expression (Zahniser and Doolen, 2001; Robinson, 2002; Quick et al., 2004) with the possibility of homeostatic regulation of GABA metabolism and of vesicular GABA content in the α1 knock-out mice (Ponomarev et al., 2006), the temporal sequence may be different and other events may be involved.

Regarding reversibility of neurotransmitter transporters (Levi and Raiteri, 1993; Gaspary et al., 1998; Richerson and Wu, 2003), we and others (Rossi et al., 2003) find no evidence that transporter reversal significantly contributes to increase extracellular [GABA] in the CGC layer. There remains a possibility that we could not detect a small fraction of GATs operating in the reversed manner in response to narrowly localized differences in concentration gradients of the transported ions.

Our biochemical analyses indicate that membrane-bound

GAT protein levels are not significantly different between the genotypes. Although a change in GAT protein may be below the levels of Western blot and biotinylation assays resolution, a change in GAT protein expression is not required for a change in GAT uptake capacity (Sutch et al., 1999; Zahniser and Doolen, 2001; Fueta et al., 2003; Quick et al., 2004). Similar to our findings, Sutch et al. (1999) reported a reduction of GAT-1 activity without changes in the number of these proteins in Genetic Absence Epilepsy Rats from Strasbourg. Regulation of extracellular [GABA] by GATs, however, is complicated by evidence that extracellular [GABA] can in turn regulate GAT activity (Bernstein and Quick, 1999). Our rough estimate of increase of ambient [GABA] in the α1 knock-out is on the order of 100–200 nM (based on currents elicited by BIC and low [GABA]). It is likely that this relatively small increase in [GABA] is not sufficient to activate the upregulation mechanism for GAT-mediated transport.

Lack of a large portion of synaptic receptors and a 20% reduction of GAT activity can be speculated to introduce an imbalance of control over extracellular [GABA]. In light of such imbalance, the short single-channel open times and insensitivity to increasing [GABA] in the α1 $^{-/-}$ may play a role of stabilizing the inhibitory drive over a range of GABA concentrations.

Of note is the fact that mouse GAT-1 knock-out mice (Chiu et al., 2005) exhibit a slight tremor similar to the one reported in the α1 $^{-/-}$ mice (Kralic et al., 2002, 2005). Of additional interest is that various epilepsy models are associated with decreased GAT activity (During et al., 1995; Sutch et al., 1999; Patrylo et al., 2001; Fueta et al., 2003). The presence of a physiologically relevant tremor in this knock-out model (Kralic et al., 2005) together with decreased GAT activity and increased extracellular [GABA] add a line of evidence with a potential for understanding regulation of neuronal excitability in pathological states.

In conclusion, we identify tonic GABAergic current as a novel compensatory mechanism in the CGCs of mice lacking the α1 subunit of the GABA$_A$ receptor and provide evidence that GAT activity could serve as a highly sensitive regulator of neuronal excitability.

References

Belelli D, Peden DR, Rosahl TW, Wafford KA, Lambert JJ (2005) Extrasynaptic GABA$_A$ receptors of thalamocortical neurons: a molecular target for hypnotics. J Neurosci 25:11513–11520.

Bernstein EM, Quick MW (1999) Regulation of gamma-aminobutyric acid (GABA) transporters by extracellular GABA. J Biol Chem 274:889–895.

Brickley SG, Cull-Candy SG, Farrant M (1996) Development of a tonic form of synaptic inhibition in rat cerebellar granule cells resulting from persistent activation of GABAA receptors. J Physiol (Lond) 497:753–759.

Brickley SG, Revilla V, Cull-Candy SG, Wisden W, Farrant M (2001) Adaptive regulation of neuronal excitability by a voltage-independent potassium conductance. Nature 409:88–92.

Brickley SG, Cull-Candy SG, Farrant M (2003) Vesicular release of GABA contributes to both phasic and tonic inhibition of granule cells in the mature cerebellum of mice. J Physiol (Lond) 547P:C30.

Brown N, Kerby J, Bonnert TP, Whiting PJ, Wafford KA (2002) Pharmacological characterization of a novel cell line expressing human $\alpha_4\beta_3\delta$ GABA$_A$ receptors. Br J Pharmacol 136:965–974.

Chiu CS, Brickley S, Jensen K, Southwell A, Mckinney S, Cull-Candy S, Mody I, Lester HA (2005) GABA transporter deficiency causes tremor, ataxia, nervousness, and increased GABA-induced tonic conductance in cerebellum. J Neurosci 25:3234–3245.

Cope DW, Hughes SW, Crunelli V (2005) GABA$_A$ receptor-mediated tonic inhibition in thalamic neurons. J Neurosci 25:11553–11563.

Crestani F, Assandri R, Tauber M, Martin JR, Rudolph U (2002) Contribution of the alpha1-GABA$_A$ receptor subtype to the pharmacological actions of benzodiazepine site inverse agonists. Neuropharmacology 43:679–684.

Ducic I, Caruncho HJ, Zhu WJ, Vicini S, Costa E (1995) γ-Aminobutyric acid gating of Cl $^-$ channels in recombinant GABA$_A$ receptors. J Pharmacol Exp Ther 272:438–445.

During MJ, Ryder KM, Spencer DD (1995) Hippocampal GABA transporter function in temporal-lobe epilepsy. Nature 376:174–177.

Ebert B, Thompson SA, Saounatsou K, McKernan R, Krogsgaard-Larsen P, Wafford KA (1997) Differences in agonist/antagonist binding affinity and receptor transduction using recombinant human γ-aminobutyric acid type A receptors. Mol Pharmacol 52:1150–1156.

Farrant M, Nusser Z (2005) Variations on an inhibitory theme: phasic and tonic activation of GABA$_A$ receptors. Nat Rev Neurosci 6:215–229.

Fisher JL (2004) The α1 and α6 subunit subtypes of the mammalian GABA$_A$ receptor confer distinct channel gating kinetics. J Physiol (Lond) 561:433–448.

Fisher JL, Macdonald RL (1997) Single channel properties of recombinant GABA$_A$ receptors containing γ2 or δ subtypes expressed with α1 and β3 subtypes in mouse L929 cells. J Physiol (Lond) 505:283–297.

Fritschy JM, Paysan J, Enna A, Mohler H (1994) Switch in the expression of rat GABA$_A$-receptor subtypes during postnatal development: an immunohistochemical study. J Neurosci 14:5302–5324.

Fueta Y, Vasilets LA, Takeda K, Kawamura M, Schwarz W (2003) Downregulation of GABA-transporter function by hippocampal translation products: its possible role in epilepsy. Neuroscience 118:371–378.

Gaspary HL, Wang W, Richerson GB (1998) Carrier-mediated GABA release activates GABA receptors on hippocampal neurons. J Neurophysiol 80:270–281.

Gingrich KJ, Roberts WA, Kass RS (1995) Dependence of the GABA$_A$ receptor gating kinetics on the alpha-subunit isoform: implications for structure-function relations and synaptic transmission. J Physiol (Lond) 489:529–543.

Hamann M, Rossi DJ, Attwell D (2002) Tonic and spillover inhibition of granule cells control information flow through cerebellar cortex. Neuron 33:625–633.

Hanchar HJ, Dodson PD, Olsen RW, Otis TS, Wallner M (2005) Alcohol-induced motor impairment caused by increased extrasynaptic GABA$_A$ receptor activity. Nat Neurosci 8:339–345.

Heinen K, Baker RE, Spijker S, Rosahl T, van Pelt J, Brussaard AB (2003) Impaired dendritic spine maturation in GABA$_A$ receptor α1 subunit knock out mice. Neuroscience 122:699–705.

Hevers W, Luddens H (2002) Pharmacological heterogeneity of γ-aminobutyric acid receptors during development suggests distinct classes of rat cerebellar granule cells in situ. Neuropharmacology 42:34–47.

Hinkle DJ, Macdonald RL (2003) β subunit phosphorylation selectively increases fast desensitization and prolongs deactivation of α1β1γ2L and α1β3γ2L GABA$_A$ receptor currents. J Neurosci 23:11698–11710.

Itouji A, Sakai N, Tanaka C, Saito N (1996) Neuronal and glial localization of two GABA transporters (GAT1 and GAT3) in the rat cerebellum. Brain Res Mol Brain Res 37:309–316.

Jones A, Korpi ER, McKernan RM, Pelz R, Nusser Z, Makela R, Mellor JR, Pollard S, Bahn S, Stephenson FA, Randall AD, Sieghart W, Somogyi P, Smith AJ, Wisden W (1997) Ligand-gated ion channel subunit partnerships: GABA$_A$ receptor α6 subunit gene inactivation inhibits δ subunit expression. J Neurosci 17:1350–1362.

Jovanovic JN, Thomas P, Kittler JT, Smart TG, Moss SJ (2004) Brain-derived neurotrophic factor modulates fast synaptic inhibition by regulating GABA$_A$ receptor phosphorylation, activity, and cell-surface stability. J Neurosci 24:522–530.

Kralic JE, Korpi ER, O'Buckley TK, Homanics GE, Morrow AL (2002) Molecular and pharmacological characterization of GABA$_A$ receptor α1 subunit knockout mice. J Pharmacol Exp Ther 302:1037–1045.

Kralic JE, Criswell HE, Osterman JL, O'Buckley TK, Wilkie ME, Matthews DB, Hamre K, Breese GR, Homanics GE, Morrow AL (2005) Genetic essential tremor in γ-aminobutyric acidA receptor α1 subunit knockout mice. J Clin Invest 115:774–779.

Kralic JE, Sidler C, Parpan F, Homanics GE, Morrow AL, Fritschy JM (2006) Compensatory alteration of inhibitory synaptic circuits in cerebellum and thalamus of γ-aminobutyric acid type A receptor α1 subunit knockout mice. J Comp Neurol 495:408–421.

Laurie DJ, Seeburg PH, Wisden W (1992) The distribution of 13 GABA$_A$ receptor subunit mRNAs in the rat brain. II. Olfactory bulb and cerebellum. J Neurosci 12:1063–1076.

Lavoie AM, Tingey JJ, Harrison NL, Pritchett DB, Twyman RE (1997) Activation and deactivation rates of recombinant GABA_A receptor channels are dependent on alpha-subunit isoform. Biophys J 73:2518–2526.

Levi G, Raiteri M (1993) Carrier-mediated release of neurotransmitters. Trends Neurosci 16:415–419.

Maguire JL, Stell BM, Rafizadeh M, Mody I (2005) Ovarian cycle-linked changes in GABA_A receptors mediating tonic inhibition alter seizure susceptibility and anxiety. Nat Neurosci 8:797–804.

Mitchell SJ, Silver RA (2003) Shunting inhibition modulates neuronal gain during synaptic excitation. Neuron 38:433–445.

Mozrzymas JW, Zarnowska ED, Pytel M, Mercik K (2003) Modulation of GABA_A receptors by hydrogen ions reveals synaptic GABA transient and a crucial role of the desensitization process. J Neurosci 23:7981–7992.

Murase K, Ryu PD, Randic M (1989) Excitatory and inhibitory amino acids and peptide-induced responses in acutely isolated rat spinal dorsal horn neurons. Neurosci Lett 103:56–63.

Nusser Z, Sieghart W, Somogyi P (1998) Segregation of different GABA_A receptors to synaptic and extrasynaptic membranes of cerebellar granule cells. J Neurosci 18:1693–1703.

Nusser Z, Sieghart W, Mody I (1999) Differential regulation of synaptic GABA_A receptors by cAMP-dependent protein kinase in mouse cerebellar and olfactory bulb neurones. J Physiol (Lond) 521:421–435.

Ogris W, Lehner R, Fuchs K, Furtmuller B, Hoger H, Homanics GE, Sieghart W (2006) Investigation of the abundance and subunit composition of GABA receptor subtypes in the cerebellum of α1-subunit-deficient mice. J Neurochem 96:136–147.

Ortinski PI, Lu C, Takagaki K, Fu Z, Vicini S (2004) Expression of distinct alpha subunits of GABA_A receptor regulates inhibitory synaptic strength. J Neurophysiol 92:1718–1727.

Patrylo PR, Spencer DD, Williamson A (2001) GABA uptake and heterotransport are impaired in the dentate gyrus of epileptic rats and humans with temporal lobe sclerosis. J Neurophysiol 85:1533–1542.

Ponomarev I, Maiya R, Harnett MT, Schafer GL, Ryabinin AE, Blednov YA, Morikawa H, Boehm II SL, Homanics GE, Berman A, Lodowski KH, Bergeson SE, Adron Harris R (2006) Transcriptional signatures of cellular plasticity in mice lacking the α1 subunit of GABA_A receptors. J Neurosci 26:5673–5683.

Pow DV, Sullivan RK, Williams SM, Scott HL, Dodd PR, Finkelstein D (2005) Differential expression of the GABA transporters GAT-1 and GAT-3 in brains of rats, cats, monkeys and humans. Cell Tissue Res 320:379–392.

Pytel M, Mercik K, Mozrzymas JW (2005) Membrane voltage modulates the GABA_A receptor gating in cultured rat hippocampal neurons. Neuropharmacology 50:143–153.

Quick MW, Hu J, Wang D, Zhang HY (2004) Regulation of a γ-aminobutyric acid transporter by reciprocal tyrosine and serine phosphorylation. J Biol Chem 279:15961–15967.

Reynolds DS, O'Meara GF, Newman RJ, Bromidge FA, Atack JR, Whiting PJ, Rosahl TW, Dawson GR (2003) GABA_A α1 subunit knock-out mice do not show a hyperlocomotor response following amphetamine or cocaine treatment. Neuropharmacology 44:190–198.

Richerson GB, Wu Y (2003) Dynamic equilibrium of neurotransmitter transporters: not just for reuptake anymore. J Neurophysiol 90:1363–1374.

Robinson MB (2002) Regulated trafficking of neurotransmitter transporters: common notes but different melodies. J Neurochem 80:1–11.

Rossi DJ, Hamann M (1998) Spillover-mediated transmission at inhibitory synapses promoted by high affinity α6 subunit GABA_A receptors and glomerular geometry. Neuron 20:783–795.

Rossi DJ, Hamann M, Attwell D (2003) Multiple modes of GABAergic inhibition of rat cerebellar granule cells. J Physiol (Lond) 548:97–110.

Rudolph U, Mohler H (2004) Analysis of GABA_A receptor function and dissection of the pharmacology of benzodiazepines and general anesthetics through mouse genetics. Annu Rev Pharmacol Toxicol 44:475–498.

Rudolph U, Crestani F, Benke D, Brunig I, Benson JA, Fritschy JM, Martin JR, Bluethmann H, Mohler H (1999) Benzodiazepine actions mediated by specific γ-aminobutyric acid_A receptor subtypes. Nature 401:796–800.

Saxena NC, Macdonald RL (1994) Assembly of GABAA receptor subunits: role of the δ subunit. J Neurosci 14:7077–7086.

Saxena NC, Macdonald RL (1996) Properties of putative cerebellar γ-aminobutyric acid A receptor isoforms. Mol Pharmacol 49:567–579.

Scimemi A, Semyanov A, Sperk G, Kullmann DM, Walker MC (2005) Multiple and plastic receptors mediate tonic GABA_A receptor currents in the hippocampus. J Neurosci 25:10016–10024.

Semyanov A, Walker MC, Kullmann DM (2003) GABA uptake regulates cortical excitability via cell type-specific tonic inhibition. Nat Neurosci 6:484–490.

Semyanov A, Walker MC, Kullmann DM, Silver RA (2004) Tonically active GABA_A receptors: modulating gain and maintaining the tone. Trends Neurosci 27:262–269.

Sigworth FJ, Sine SM (1987) Data transformations for improved display and fitting of single-channel dwell time histograms. Biophys J 52:1047–1054.

Sur C, Wafford KA, Reynolds DS, Hadingham KL, Bromidge F, Macaulay A, Collinson N, O'Meara G, Howell O, Newman R, Myers J, Atack JR, Dawson GR, McKernan RM, Whiting PJ, Rosahl TW (2001) Loss of the major GABA_A receptor subtype in the brain is not lethal in mice. J Neurosci 21:3409–3418.

Sutch RJ, Davies CC, Bowery NG (1999) GABA release and uptake measured in crude synaptosomes from genetic absence epilepsy rats from Strasbourg (GAERS). Neurochem Int 34:415–425.

Uusi-Oukari M, Heikkila J, Sinkkonen ST, Makela R, Hauer B, Homanics GE, Sieghart W, Wisden W, Korpi ER (2000) Long-range interactions in neuronal gene expression: evidence from gene targeting in the GABA_A receptor β2-α6-α1-γ2 subunit gene cluster. Mol Cell Neurosci 16:34–41.

Vicini S, Ortinski P (2004) Genetic manipulations of GABA_A receptor in mice make inhibition exciting. Pharmacol Ther 103:109–120.

Vicini S, Ferguson C, Prybylowski K, Kralic J, Morrow AL, Homanics GE (2001) GABA_A receptor α1 subunit deletion prevents developmental changes of inhibitory synaptic currents in cerebellar neurons. J Neurosci 21:3009–3016.

Wadiche JI, Jahr CE (2005) Patterned expression of Purkinje cell glutamate transporters controls synaptic plasticity. Nat Neurosci 8:1329–1334.

Wall MJ (2005) Alterations in GABA_A receptor occupancy occur during the postnatal development of rat Purkinje cell but not granule cell synapses. Neuropharmacology 49:596–609.

Wall MJ, Usowicz MM (1997) Development of action potential-dependent and independent spontaneous GABA_A receptor-mediated currents in granule cells of postnatal rat cerebellum. Eur J Neurosci 9:533–548.

Wisden W, Laurie DJ, Monyer H, Seeburg PH (1992) The distribution of 13 GABAA receptor subunit mRNAs in the rat brain. I. Telencephalon, diencephalon, mesencephalon. J Neurosci 12:1040–1062.

Wu Y, Wang W, Richerson GB (2003) Vigabatrin induces tonic inhibition via GABA transporter reversal without increasing vesicular GABA release. J Neurophysiol 89:2021–2034.

Zahniser NR, Doolen S (2001) Chronic and acute regulation of Na^+/Cl^--dependent neurotransmitter transporters: drugs, substrates, presynaptic receptors, and signaling systems. Pharmacol Ther 92:21–55.